

## Study of the $^{17}\text{O}(n,\alpha)^{14}\text{C}$ reaction: extension of the Trojan Horse Method to neutron induced reactions

---

### **Giovanni Luca Guardo<sup>1</sup>**

*Università degli Studi di Catania & INFN – Laboratori Nazionali del Sud  
Catania, Italy*

*E-mail: [guardo@lns.infn.it](mailto:guardo@lns.infn.it)*

### **Livio Lamia**

*Università degli Studi di Catania & INFN – Laboratori Nazionali del Sud  
Catania, Italy*

*E-mail: [llamia@lns.infn.it](mailto:llamia@lns.infn.it)*

### **Claudio Spitaleri**

*Università degli Studi di Catania & INFN – Laboratori Nazionali del Sud  
Catania, Italy*

*E-mail: [spitaleri@lns.infn.it](mailto:spitaleri@lns.infn.it)*

### **Xiao-Dong Tang**

*University of Notre Dame  
South Bend (IN), USA*

### **Shawn Brian**

*University of Notre Dame  
South Bend (IN), USA*

### **Brian Bucher**

*University of Notre Dame  
South Bend (IN), USA*

### **Manoel Couder**

*University of Notre Dame  
South Bend (IN), USA*

### **Paul Davies**

*University of Notre Dame  
South Bend (IN), USA*

### **Richard deBoer**

*University of Notre Dame  
South Bend (IN), USA*

---

<sup>1</sup> Speaker

**Marisa Gulino**

*INFN – Laboratori Nazionali del Sud  
Catania, Italy*

**Marco La Cognata**

*INFN – Laboratori Nazionali del Sud  
Catania, Italy*

**Larry Lamm**

*University of Notre Dame  
South Bend (IN), USA*

**C. Ma**

*University of Notre Dame  
South Bend (IN), USA*

**Jaromir Mrazek**

*Nuclear Physics Institute of ASCR  
Rez, Czech Republic*

**Akram Mukhamedzhanov**

*Cyclotron Institute, Texas A&M University  
College Station (TX), USA*

**Masahiro Notani**

*University of Notre Dame  
South Bend (IN), USA*

**Rosario Gianluca Pizzone**

*INFN – Laboratori Nazionali del Sud  
Catania, Italy*

**Giuseppe Rapisarda**

*INFN – Laboratori Nazionali del Sud  
Catania, Italy*

**Daniel Robertson**

*University of Notre Dame  
South Bend (IN), USA*

**Maria Letizia Sergi**

*INFN – Laboratori Nazionali del Sud  
Catania, Italy*

**Wanpeng Tan**

*University of Notre Dame  
South Bend (IN), USA*

Neutron induced reactions play a key role in several astrophysical scenario. In particular, the importance of  $^{17}\text{O}(n,\alpha)^{14}\text{C}$  reaction is twofold: in the Inhomogeneous Big Bang Nucleosynthesis (*IBBN*), in which  $^{14}\text{C}$  may act as a bottleneck in the heavy-element production, and during the weak component of the s-process, for which the determination of the ratio between the  $^{17}\text{O}(\alpha,n)^{20}\text{Ne}$  and  $^{17}\text{O}(n,\alpha)^{14}\text{C}$  reaction rates is important to pin down the neutron flux for the nucleosynthesis. The experimental study of the  $^{17}\text{O}(n,\alpha)^{14}\text{C}$  reaction has been performed in the energy range 0-350 keV via the Trojan Horse Method (*THM*). The reaction has been deduced by applying the THM to the  $^2\text{H}(^{17}\text{O},\alpha)^{14}\text{C}^1\text{H}$  quasi-free reaction induced at the laboratory energy of 43.5 MeV, using deuteron as the Trojan Horse nucleus. The preliminary results show that the contribution of the 166 keV and 236 keV resonances is in energy agreement with the available direct data. A clear contribution of the -7 keV subthreshold level is also apparent. Moreover, this TH measurement allows one to study the  $\ell=3$ , 75 keV resonance ( $E^*=8.125$  MeV,  $J^\pi=5^-$ ) suppressed in the  $^{17}\text{O}(n,\alpha)^{14}\text{C}$  direct measurements.

*VI European Summer School on Experimental Nuclear Astrophysics  
Acireale Italy  
September 18-27, 2011*

## 1. Introduction

Recent studies have shown the role of the  $^{17}\text{O}(n,\alpha)^{14}\text{C}$  reaction during the primordial nucleosynthesis in the framework of Inhomogeneous Big Bang Nucleosynthesis (*IBBN*). In [1-2] the authors suggest that it is possible to identify an enhanced baryon density zone and a less dense baryon zone. The baryon to photon ratio  $\eta$  is then fixed in average between the 2 zones to the value of  $6.2 \pm 0.2 \cdot 10^{-10}$  [3] deduced from WMAP measurements. In the high density region, the  $^{14}\text{C}$  abundance increases from  $10^{-12}$  to  $\sim 7 \cdot 10^{-7}$  mass fraction [4]. Once produced, carbon could activate the network leading to  $^{22}\text{Ne}$ :



a fundamental element for the production of heavy elements.

A major  $^{14}\text{C}$  synthesis channel is the  $^{17}\text{O}(n,\alpha)^{14}\text{C}$  reaction, in the energy range 0-200 keV, corresponding to the temperature that characterize the model:  $0.7 \cdot 10^9 < T < 1 \cdot 10^9$  K.

In massive stars (with initial mass  $M > 8M_{\odot}$ ), the  $^{17}\text{O}(n,\alpha)^{14}\text{C}$  reaction may act as a neutron poison reducing the neutron flux available for the so called weak s-process [5]. In such stars, the main neutron source is provided by the  $^{22}\text{Ne}(\alpha,n)^{25}\text{Mg}$  reaction, activated at the end of the convective core He-burning and in the following convective shell C-burning [6]. However, the He-core is enriched in oxygen because of the CNO cycle, thus an ignition of the  $^{16}\text{O}(n,\gamma)^{17}\text{O}$  reaction is also expected. The produced  $^{17}\text{O}$  can experience both  $(\alpha,n)$  or  $(n,\alpha)$  reactions. The  $^{17}\text{O}(\alpha,n)^{20}\text{Ne}$  reaction represents a recycle channel for the neutron flux while the  $^{17}\text{O}(n,\alpha)^{14}\text{C}$  reaction is a neutron poison reaction. Therefore the knowledge of the ratio between the cross section of these reactions is important to determine the neutron flux available for the s-process.

For these reasons, a detailed measurement of the cross section in the energy range from 0 up to a few hundreds keV is needed. In this energy region, several  $^{18}\text{O}$  states contribute to the total cross section, thus a careful evaluation of their strengths is needed [7]. However, only few direct measurements are reported in the literature, showing discordances in the energy range of interest [8-11].

The aim of this work is to show how the application of the indirect Trojan Horse Method (THM) [12-13] allows one to use the deuteron quasi-free (QF) break-up as a source of virtual neutrons and to overcome the effects of the centrifugal barrier.

## 2. The Trojan Horse Method

The TH method has been developed in the early 1990s with the aim of measuring low-energy nuclear reactions hindered by the Coulomb barrier and, since then, it has been successfully applied to several reactions of astrophysical interest [14-15]. Recently, this approach has been extended to the neutron induced reactions starting with the  $^6\text{Li}(n,\alpha)^3\text{H}$  reaction [16].

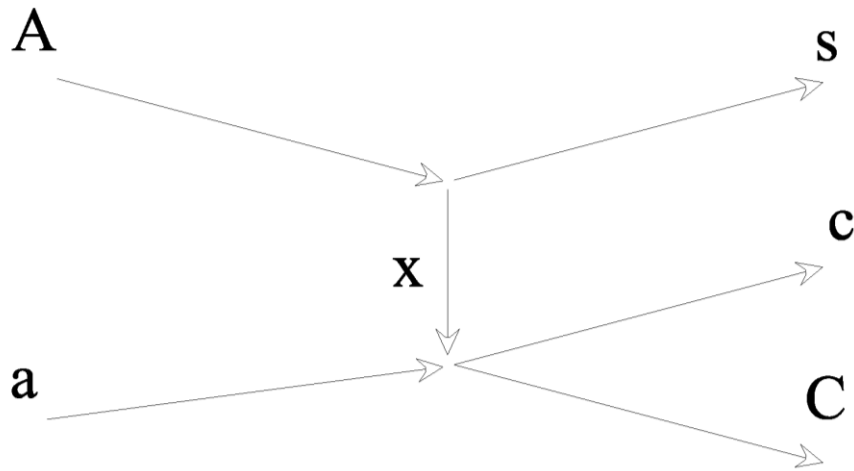


**Figure 1** – Pole diagram describing the QF mechanisms discussed in the text.

Basically, the QF break-up mechanisms are direct processes in which the interaction between an impinging nucleus and the target can cause the break-up of the target (TBU) or, that is the same, of the projectile (PBU) [17]. In particular, the so called QF processes have three particles in the exit channel, one of which can be thought as “spectator”.

In the case of TBU, an interaction between the impinging nucleus and a fraction of the nucleons forming the target (called “participant”) takes place, while the others does not participate to the reaction. The spectator is emitted without interacting with the incoming nucleus or the participants.

The analysis of the QF reactions is usually performed in the framework of the Impulse Approximation (IA) [18], for which, by assuming the  $A = x \oplus s$  cluster configuration, the QF  $A + a \rightarrow c + C + s$  process can be described through the pole diagram in Figure 1. The upper vertex refers to the target-nucleus break-up into  $x + s$ , while the lower vertex to the virtual two-body reaction  $a + x \rightarrow c + C$  leaving  $s$  as a spectator. In the Plane Wave Impulse Approximation approach the three-body cross section [19]

$$\frac{d^3\sigma}{dE_c d\Omega_c d\Omega_C} \propto KF |\Phi(p_S)|^2 \left( \frac{d\sigma}{d\Omega} \right)^{HOES} \quad (2)$$

where KF is a kinematical factor containing the final-state phase-space factor and it is a function of masses, momenta and angles of the outgoing particles,  $\Phi(p_s)$  is the Fourier transform of the radial wave function for the  $x$ - $s$  intercluster motion inside A and  $(d\sigma/d\Omega)^{HOES}$  is the half-off energy shell cross section. For a more focused description of the method, see [13-14,16].

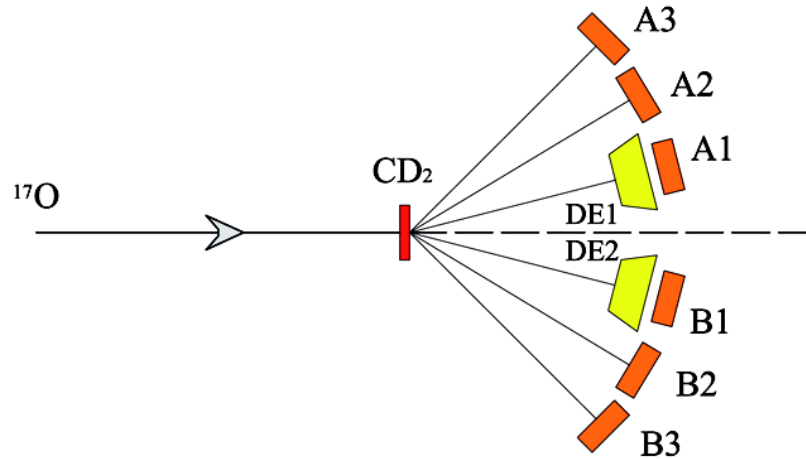


**Figure 2** – Schematic view of the experimental setup. The  $^{17}\text{O}$  beam impinging on a  $\text{CD}_2$  target. The emitted particles were detected by four PSDs (A2, A3, B2 and B3) and by two  $\Delta\text{E}$ -E telescopes (DE1-A1 and DE2-B1).

### 3. The experiment

The  $^{17}\text{O}(n,\alpha)^{14}\text{C}$  reaction has been studied via the three-body  $^2\text{H}(^{17}\text{O},\alpha)^{14}\text{C}$  reaction. The experiment was performed at the Institute for Structure and Nuclear Astrophysics (ISNAP) at the University of Notre Dame, South Bend (Indiana, USA). The JN Tandem Van der Graaff provided a 43.5 MeV  $^{17}\text{O}$  beam impinging on a deuterated polyethylene target ( $\text{CD}_2$ ) of about  $150\ \mu\text{g}/\text{cm}^2$  placed at  $90^\circ$  with respect to the beam direction. A schematical view of the used detection setup is shown in Figure 2. It was chosen to cover the phase-space region where a strong contribution of the QF reaction mechanism is expected.

Four  $500\ \mu\text{m}$  thick Position Sensitive Detectors (PSD) referred to as A2, A3, B2 and B3 and two telescopes, made up of a ionization chamber (IC) as  $\Delta\text{E}$  and a  $1000\ \mu\text{m}$  PSD (A1 and B1) as E detector, were employed. A2 and B2 were placed at a distance  $d_2=476\ \text{mm}$  and  $d_5=494\ \text{mm}$  from the target, covering the angular ranges  $17.5^\circ\pm 2.5^\circ$  while A3 and B3 were placed at  $d_3=381\ \text{mm}$  and  $d_6=405\ \text{mm}$  from the target covering the angular range  $27.3^\circ\pm 3.5^\circ$ . Finally, the two telescopes were placed at a distance  $d_1=464\ \text{mm}$  and  $d_4=495\ \text{mm}$  from the target, and they covered the angular range  $7.5^\circ \pm 2.5^\circ$ . The ICs, filled with about 50 mbar isobutane gas, had an energy resolution of  $\sim 10\%$ , which was enough to discriminate particles by their charge but not their mass. Two thin mylar foils respectively of  $0.9\ \mu\text{m}$  and  $1.5\ \mu\text{m}$  were used as entrance and exit windows of each IC. Their thickness was chosen to minimize the angular straggling. The telescopes were optimized for  $^{14}\text{C}$  detection while the other PSDs for alpha particles.

Energy and position signals for the detected particles were processed by standard electronics and sent to the acquisition system, allowing for on-line monitoring of the experiment and the data storage for off-line analysis. The logic AND between one of the two telescopes and the logic OR of the PSDs on the other side of the beam was used as trigger for the ACQ system.

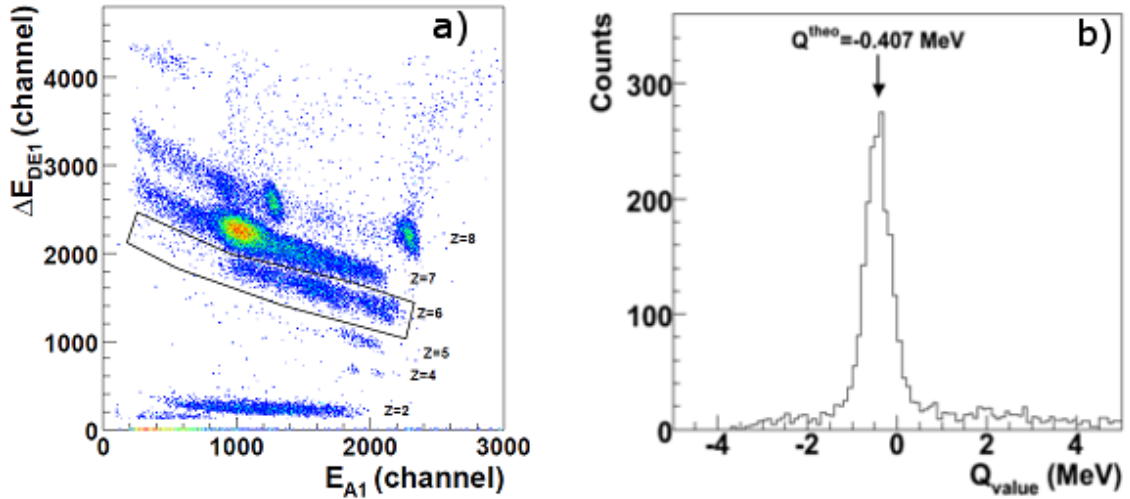


**Figure 3** –  $\Delta E$ -E matrix for C identification in the A1 telescope (a) and experimental  $Q_{\text{value}}$  of the  $^2\text{H}(^{17}\text{O},\alpha)^{14}\text{C}$  reaction in agreement with the theoretical prediction of -0.407 MeV (b).

#### 4. Data analysis and results

To perform angular calibrations, an equally spaced grid was mounted in front of each PSD and the angular position of each slit determined by using an optical system. Position and energy calibration runs were then performed by using  $^4\text{He}$  and  $^{12}\text{C}$  beams on a  $93\mu\text{g}/\text{cm}^2$  thick  $^{197}\text{Au}$  target at energies from 5 up to 50 MeV, to measure the elastic scattering peaks at several energies.

After detector calibration, the first step of the TH-analysis has been to discriminate the three-body  $^2\text{H}(^{17}\text{O},\alpha)^{14}\text{C}$  reaction of interest from others, induced by the interaction of  $^{17}\text{O}$  with other elements in the target (C, H, O, for instance). Carbon isotopes have been selected by means of the standard  $\Delta E$ -E technique. Figure 3a) shows a typical  $\Delta E$ -E plot and the C selection used for the further analysis.

By means of the energy conservation law, the experimental Q-value spectrum for the selected events was also reconstructed (Figure 3b). A good agreement with the expected value  $Q_{\text{theo}} = -0.407$  MeV for the  $^{14}\text{C} + \alpha + p$  exit channel of interest is obtained, under the hypothesis of mass number 1 for the undetected third particle. This, within the experimental uncertainties, is a signature of an accurate calibration and a precise selection of the  $^2\text{H}(^{17}\text{O},\alpha)^{14}\text{C}$  reaction.

After the identification of the 3-body channel of interest, it is necessary to discriminate the QF reaction mechanism from other reaction mechanisms, such as sequential decay and direct break-up, feeding the same particles in the final state. To this aim, relative energy correlation plots for any two of the three outgoing particles have been studied. These plots (Figure 4) show very clear vertical loci due to the excitation of the compound  $^{18}\text{O}$  nucleus. Indeed, if a  $^{18}\text{O}$  state is populated, an increase in the statistic for fixed  $E_{\text{c.m.}} = E_{\alpha^{14}\text{C}} - Q_2$  is expected, where  $E_{\alpha^{14}\text{C}}$  is the relative energy between the detected  $\alpha$  and  $^{14}\text{C}$  and  $Q_2 = 1.817$  MeV is the  $^{17}\text{O}(n,\alpha)^{14}\text{C}$  Q-value. Two horizontal loci, corresponding to  $^{15}\text{N}$  excited levels, are also detectable in a energy region far from the one of interest ( $E_{\text{c.m.}} < 0.5$  MeV), thus no subtraction of the sequential decay contribution from the coincidence yield has been necessary.

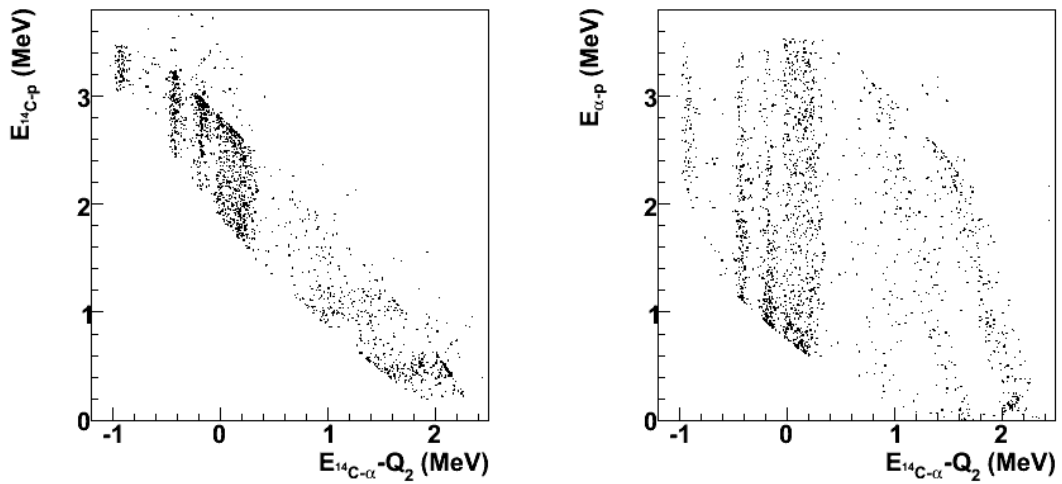


Figure 4 – Correlation spectra between the relative energy  $E_{14\text{C-p}} - E_{\text{cm}}$  and  $E_{\alpha\text{-p}} - E_{\text{cm}}$ .

On the contrary no evidence of the population  $^5\text{Li}$  levels was detected.

While  $^{15}\text{N}$  levels are populated through a sequential mechanism, a further analysis is required to find out whether  $^{18}\text{O}$  states should be attributed to sequential decay of QF process. An observable sensitive to the reaction mechanism is the momentum distribution for the relative p-n motion inside deuteron as this is a necessary condition for the occurrence of QF breakup. Therefore, the experimental momentum distribution has been determined following the standard procedure described in [16]. Selecting a small phase-space region where the two-body cross section can be assumed almost constant, the three-body coincidence yield corrected for the phase-space factor will be proportional to the momentum distribution. The experimental result is shown in Figure 5, where the coincidence yield for the events in the energy window  $E_{\text{cm}} = 166 \pm 40 \text{ keV}$ , corrected for the phase-space factor, is shown. The good agreement, within  $|p_s| < 40 \text{ MeV/c}$ , between the experimental data and the theoretical Hulthén function for the n-p relative motion is an experimental evidence that the proton acted as a “spectator” during the break-up occurred in the  $^2\text{H}(^{17}\text{O}, \alpha^{14}\text{C})\text{p}$  reaction.

After the QF selection, the experimental coincidence yield (Figure 6) has been studied. It was obtained by dividing the selected coincidence yield by the product of the phase-space factor and of the p-n momentum distribution [13].

The experimental data reported as full dots in Figure 6 clearly show the presence of four resonances corresponding to  $^{18}\text{O}$  states at 8.039 MeV, 8.125 MeV, 8.213 MeV and 8.282 MeV.

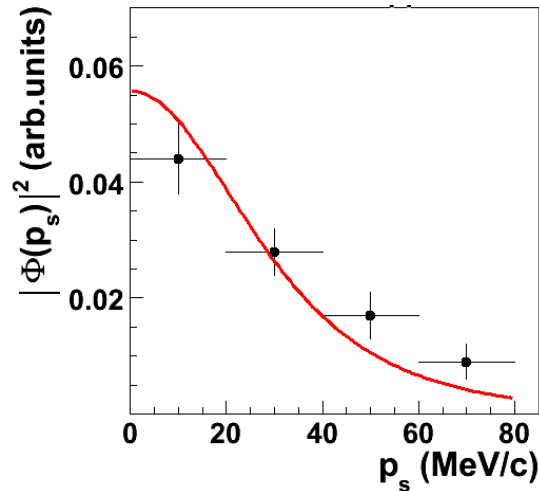


**Figure 5** – Experimental distribution (black points) for the proton-momentum values compared with the theoretical Hulthén distribution (red line). The agreement is a necessary condition for the presence of the QF-mechanism in the data.

The yield has been fitted, then, by means of the incoherent sum of four Gauss functions. For each function, the standard deviation and the normalization constant have been left as free parameters. The curves are shown as red dashed lines while the sum of these resonant terms is displayed by a black solid line. The horizontal error bars give the width of the  $^{17}\text{O}$ - $n$  relative energy bins used in the data analysis and the vertical bars show the statistical uncertainties only ( $\sim 15\%$ ).

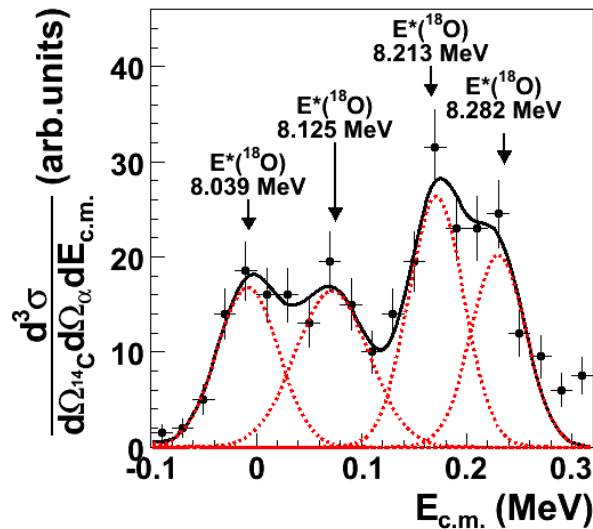


**Figure 6** – Experimental triple differential cross section of the  $^{17}\text{O}(n,\alpha)^{14}\text{C}$  reaction. The black line is a fit with four Gaussians, showed as red dashed lines.

## 5. Conclusions and future perspectives

In this work, the  $^{17}\text{O}(n,\alpha)^{14}\text{C}$  reaction has been investigated by means of the THM applied to the  $^2\text{H}(^{17}\text{O},\alpha^{14}\text{C})^1\text{H}$  process. This is an extension of the THM to the neutron induced

reactions. From such measurement, it was possible to excite the subthreshold level centered at - 7 keV in the center-of-mass system corresponding to the 8.039 MeV level of  $^{18}\text{O}$ , which is important to determine the  $^{17}\text{O}(n,\alpha)^{14}\text{C}$  reaction rate. Moreover, the use of deuteron as a source of virtual neutrons allows us to populate the level centered at 75 keV in the  $^{17}\text{O}-n$  center-of-mass system corresponding to the 8.125 MeV level of the  $^{18}\text{O}$ . Due to its  $J^\pi$  assignment ( $J^\pi=5^-$ ), the population of such level is suppressed in direct measurements because of its  $\ell=3$  angular momentum. This preliminary results clearly confirms the power of the THM to overcome the centrifugal effect. Finally, the method also reproduced correctly the energy levels available in literature.

The future aim of this work is the extraction of the angular distribution and of the resonance strength of the 75 keV level (unknown in the literature) and the determination of the contribution of the subthreshold level to the total reaction rate.

## References

- [1] R. Nakamura et al., *arXiv:1007.0466v1*, 2010.
- [2] T. Kajino et al., *Nuclear Physics* **A588** (339c) 1995.
- [3] D. J. Fixen & J. C. Mather, *Astrophysical Journal* **581** (817) 2002.
- [4] J. H. Applegate et al., *Astrophysical Journal* **329** (572) 1988.
- [5] F. Kappeler et al., *arXiv:1012.5218v1*, 2010.
- [6] M. Pignatari et al., *Astrophysical Journal* **710** (1557) 2010.
- [7] F. Ajzenberg-Selove, *Nuclear Physics* **A475** (1) 1987.
- [8] R. M. Sanders, *Physical Review* **104** (1434) 1956.
- [9] P. E. Koehler & S. M. Graff, *Physical Review* **C44** (2788) 1991.
- [10] H. Schatz et al., *Astrophysical Journal* **413** (750) 1993.
- [11] J. Wagemans et al., *Physical Review* **C65** (34614) 2002.
- [12] C. Spitaleri et al., *Physical Review* **C60** (55802) 1999.
- [13] C. Spitaleri et al., *Physical Review* **C69** (55806) 2004.
- [14] G. Baur, *Physics Letters* **B178** (135) 1986.
- [15] M. La Cognata et al., *Astrophysical Journal* **708** (796) 2010.
- [16] M. Gulino et al., *Journal Physics* **G37** (125105) 2010.
- [17] M. Jain et al., *Nuclear Physics* **A153** (49) 1970.
- [18] G. F. Chew & G. C. Wick., *Physical Review* **85** (636) 1952.
- [19] I. Slaus et al., *Nuclear Physics* **A286** (67) 1977.